

# Efficient Catalytic Liquefaction of Organosolv Lignin Over Transition Metal Supported on HZSM-5

Ke Ye, Ying Liu,\* Shubin Wu,\* and Junping Zhuang

In this work, the catalytic liquefaction of eucalyptus organosolv lignin (EOL) over hydrogen type-zeolite socony mobile-five (HZSM-5) zeolite supported transition metals in an ethanol system was studied, and a cheap transition metal NiCr/HZSM-5 catalyst was prepared. Among them, nickel and chromium proved to have a good synergistic effect, which could remarkably enhance the acidity of the catalyst surface, and the catalytic effect was better than Ru-based precious metal catalysts and commercial Raney Ni catalysts. Meanwhile, the optimal reaction process of NiCr/HZSM-5 and Raney Ni catalyst for synergistic catalysis of EOL was explored. Under the optimal process conditions, the lignin liquefaction rate reached 95.9%, the monophenol yield was 8.64%, and the char content was only 2.08%. Furthermore,  $^1\text{H}$ - $^{13}\text{C}$  heteronuclear single quantum correlation nuclear magnetic resonance ( $^1\text{H}$ - $^{13}\text{C}$  HSQC NMR) showed that the  $\beta$ -O-4,  $\beta$ - $\beta$ , and  $\beta$ -5 linkages of lignin were effectively broken. Thus, a higher liquefaction rate of lignin was realized, which provided the possibility for further comprehensive utilization of lignin.

DOI: 10.15376/biores.17.2.2275-2295

Keywords: Organosolv lignin; Catalytic liquefaction; HZSM-5; Transition metal

Contact information: South China University of Technology, State Key Laboratory of Pulp and Paper Engineering, Guangzhou 510641, Guangdong, China;

\* Corresponding authors: amyliu@scut.edu.cn; shubinwu@scut.edu.cn

## INTRODUCTION

Reducing carbon dioxide emissions in the context of “carbon neutral” has become a general trend. The increasing depletion of fossil energy and the environmental problems caused by its combustion are forcing researchers to look for cleaner renewable energy sources. As a rich and renewable biomass resource in nature, lignin is also a renewable natural aromatic polymer, which has attracted increased researchers’ attention.

Lignin is a macromolecule composed of guaiacyl (G), syringyl (S), and p-hydroxyphenyl (H) structural units connected by ether bonds and C-C bonds, and the source of lignin and the method of separation have a great influence on the structure of lignin (Galkin and Samec 2016; Patil *et al.* 2020). Hardwoods with more abundant  $\beta$ -O-4 bond content and S-type monomer content were considered to be more prone to depolymerization. The organosolv process is a method of dissolving lignin in an organic solvent to separate lignin. Studies (Deuss *et al.* 2017; Rinaldi *et al.* 2016; Shu *et al.* 2016a) had shown that organosolv lignin with lower molecular weight and more unsaturated carbonyl groups were more likely to depolymerize than other lignin. Therefore, in this paper, a typical hardwood eucalyptus was used as raw material and extract eucalyptus lignin by organosolv process.

In the past, most of lignin was incinerated in the paper industry without high-value utilization. However, catalytic liquefaction technology can convert lignin into valuable monophenolic compounds and bio-oil, which is a promising way for lignin valorization (Shao *et al.* 2017; Ye *et al.* 2021; Zhang *et al.* 2020), especially in the context of the “lignin first” strategy. There have been many studies on the catalytic liquefaction of lignin. For instance, Qi *et al.* (2017) studied the effect of hydrogen peroxide pretreatment on the catalytic liquefaction of kraft lignin over Ni/ZSM-5 zeolite catalyst in alkaline water, and found that hydrogen peroxide pretreatment can oxidize the alcoholic hydroxyl groups of kraft lignin, thereby inhibiting repolymerization, and the bio-oil yield reached 83%. Kim *et al.* (2015b) studied Pt/C, Pd/C, Ru/C, Ni/C (four catalysts) in methanol, ethanol, and isopropanol (three alcohol systems) to catalyze the liquefaction of lignin to produce bio-oil, and found that the combination of different alcohols and catalysts had an important influence on the molecular weight and structure distribution of lignin depolymerization products; the combination of ethanol and Pt/C catalyst can produce 77.4% lignin oil and 3.7% char. However, these studies have the problems of complicated pretreatment processes or high costs of using precious metal catalysts.

Zeolite is often used in the catalytic liquefaction of lignin because of its special pore structure and certain surface acidity, which can promote mass transfer and ether bond cracking in the liquefaction process (Kong *et al.* 2019; Singh and Ekhe 2014a; Wang *et al.* 2018). In addition, the limited pore action can inhibit the repolymerization of small molecules. In the past, noble metal catalysts supported on zeolite have been widely reported (Wang *et al.* 2017), and compared with noble metal catalysts, transition metal catalysts have the advantages of good economy and wide sources. This paper compares the catalytic liquefaction activity differences of the five transition metals Cr, Fe, Co, Ni, and Cu supported on HZSM-5 and compares these with the noble metal Ru. The synergistic effect of supported HZSM-5 zeolite catalyst and Raney nickel catalyst also was studied.

## EXPERIMENTAL

### Materials

Ethanol,  $\text{Cr}(\text{NO}_3)_3 \cdot 9\text{H}_2\text{O}$ ,  $\text{Fe}(\text{NO}_3)_3 \cdot 9\text{H}_2\text{O}$ ,  $\text{Co}(\text{NO}_3)_2 \cdot 6\text{H}_2\text{O}$ ,  $\text{Ni}(\text{NO}_3)_2 \cdot 6\text{H}_2\text{O}$ ,  $\text{Cu}(\text{NO}_3)_2 \cdot 3\text{H}_2\text{O}$ , and  $\text{RuCl}_3 \cdot 3\text{H}_2\text{O}$  were analytical grade and purchased from Shanghai Macklin Biochemical Co., Ltd. (Shanghai, China). Ethyl acetate ( $\geq 99.7\%$ ) was purchased from General-reagent® (Shanghai, China), and HZSM-5 was purchased from Nankai University Catalyst Co., Ltd. (Tianjin, China).

### Lignin Extraction

Eucalyptus was provided by Zhanjiang Chenming Pulp & Paper Co., Ltd. (Zhanjiang, China). These wood chips were crushed by grinder and extracted with a mixed solution of 200 mL benzene and 100 mL ethanol for 6 h after vacuum drying at 60 °C. Eucalyptus organosolv lignin (EOL) was separated according to the procedure reported in a previous study (Wen *et al.* 2013).

### Catalyst Preparation

The catalysts were prepared by impregnation methods. A certain amount of metal salts was weighed accurately and dissolved in 10 mL ultrapure water. Then 2.5 g HZSM-5 zeolite was added, sonicated for 1 h, and stirred at room temperature for 12 h. It was dried

overnight at 80 °C. The catalysts were calcined at 600 °C (10 °/min) under an O<sub>2</sub> atmosphere for 4 h and were reduced at 650 °C (10 °/min) under a H<sub>2</sub> atmosphere for 4 h prior to use.

### Catalyst Characterization

X-ray diffraction (XRD) patterns of the catalysts were observed with an X'pert Power (PANalytical, Almelo, Netherlands) device with Cu K $\alpha$  from 5 ° to 80 ° and with a scan speed of 10 °/min. A thermo scientific K-Alpha X-ray photoelectron spectrometer (XPS) (Thermo Fisher Scientific, Waltham, MA, USA) was used to analyze the surface elements and valence states of the sample, and the binding energy of organic pollution carbon C1s was 284.6 eV as a reference for binding energy correction. The N<sub>2</sub> adsorption-desorption isotherms of the catalysts were performed on Mike ASAP2460 (Micromeritics Instrument Corp, Atlanta, GA, USA) and the sample was degassed at 300 °C for 8 h before testing. The acidity of the sample surface was analyzed by NH<sub>3</sub> temperature-programmed desorption (NH<sub>3</sub>-TPD) with AutoChem II 2920 (Micromeritics Instrument Corp, Atlanta, GA, USA). The sample was dried and pretreated at 300 °C before being testing and cooled to 50 °C by He gas purging. Then, it was filled with 10% NH<sub>3</sub>/He mixed gas to saturation, switched back to the He gas to purge the weak physical adsorption of NH<sub>3</sub> on the surface, and finally it was heated up to 700 °C under He gas at a heating rate of 10 °/min for desorption.

### Catalytic Liquefaction of Organosolv Lignin

The catalytic hydrogenolysis of lignin was performed in a 100-mL high pressure vessel. Typically, 0.5 g lignin, 0.1 g catalyst, and 12 g ethanol were added in the autoclave reactor and was purged with N<sub>2</sub> five times to expel air. Then, the reactor was heated to the set temperature at a stirring speed of 500 rpm, and timing started after reaching the designed temperature.

After the reaction was completed, it was cooled down to room temperature in rapid water bath. Next, the reactor was opened and a certain amount of chlorobenzene was added as the internal standard. The liquid phase product separated by filtration was extracted with ethyl acetate, and 1 mL sample was taken for GC-MS and GC-FID analysis before rotary evaporation. Then the extracted liquid underwent 40 °C rotary evaporation to remove the solvent, and the remaining liquid products were recovered and weighed. These products were bio-oil. The solid residue that included catalyst and char was dried overnight at 80 °C and weighed. Because there was almost no gas generated in the reaction, the gas phase products were negligible.

### Characterization of Lignin and Depolymerized Products

The functional groups of raw lignin and depolymerized products were analyzed by Fourier transform infrared spectroscopy (FTIR, Thermo Fisher Scientific, Waltham, MA, USA), and the potassium bromide tablet method was used for determination. The detection conditions were as follows: the number of scans was 32, the scan range was 400 to 4000 cm<sup>-1</sup>, and the resolution was 4 cm<sup>-1</sup>. The structure of lignin was analyzed by HSQC with a Bruker AVANCE NEO 500M (Bruker, Karlsruhe, Germany). The detection conditions and analysis refer to the methods reported in the literature (Chen *et al.* 2020).

## Product Analysis

The liquid products were detected and identified by gas chromatography with a mass spectrometer (GC–MS, Agilent 7890A-5975C, Agilent Technologies, Santa Clara, CA, USA), equipped with a DB-WAX capillary column (30 m × 0.25 mm × 0.25 μm). The GC–MS working conditions were as follows: the oven temperature was kept at 40 °C for 2 min, increased to 140 °C at a rate of 20 °C/min and held for 2 min, and finally increased to 250 °C at a rate of 10 °C/min and held for 1 min. The identification of products in bio-oil was obtained by NIST14 mass library. The quantification of phenolic monomers was calculated by the internal standard method with chlorobenzene as the internal standard, and the analysis and detection were performed using gas chromatograph with a flame ionization detector (GC2014, Shimadzu Scientific Instruments, Kyoto, Japan), equipped with a DB-WAX capillary column (30 m × 0.25 mm × 0.25 μm). The GC–FID working conditions were the same as GC-MS.

The yields of bio-oil, monophenol, and char were calculated using the following Eqs. 1 through 3,

$$Y_{\text{bio-Oil}} = W_o / W_{\text{EOL}} \times 100 \quad (1)$$

$$Y_{\text{monophenol}} = W_m / W_{\text{EOL}} \times 100 \quad (2)$$

$$Y_{\text{char}} = (W_r - W_c) / W_{\text{EOL}} \times 100 \quad (3)$$

where  $Y_{\text{bio-Oil}}$  is the lignin liquefaction extent (%), as well as bio-oil yield (%),  $Y_{\text{monophenol}}$  is the yield of monophenol (%),  $Y_{\text{char}}$  is the yield of char (%),  $W_o$  is the weight (g) of bio-oil,  $W_{\text{EOL}}$  is the weight (g) of initial EOL,  $W_m$  is the weight (g) of monophenol,  $W_r$  is the weight (g) of solid residue, and  $W_c$  is the weight (g) of catalyst.

## RESULTS AND DISCUSSION

### Catalyst Characterization

The XRD diffraction patterns of HZSM-5, Cr/HZSM-5, Ni/HZSM-5, and NiCr/HZSM-5 catalysts are shown in Fig. 1.

The characteristic diffraction peak of HZSM-5 supported nickel was clearly observed at  $2\theta$  of 44.3°, 51.7°, and 76.1°, respectively, and the corresponding diffraction planes were (111), (200), and (220). The characteristic diffraction peak of HZSM-5 supported chromium was clearly observed at  $2\theta$  of 33.2°, 41.6°, 50.3°, 54.9°, 63.5°, and 65.15°, respectively, and these were the characteristic diffraction peaks of the crystalline  $\alpha$ -Cr<sub>2</sub>O<sub>3</sub> phase (Gaspar *et al.* 2005; Santhosh Kumar *et al.* 2009), indicating that the metallic nickel and chromium were successfully supported on the surface of the HZSM-5. Comparing Cr/HZSM-5, Ni/HZSM-5 single metal catalyst, and NiCr/HZSM-5 bimetallic catalyst, there were no new diffraction peaks formed, indicating that the nickel and chromium did not form an alloy phase, and all samples had typical HZSM-5 zeolite molecular sieve diffraction peaks, indicating that the supported metals did not change the structure of the HZSM-5 support.

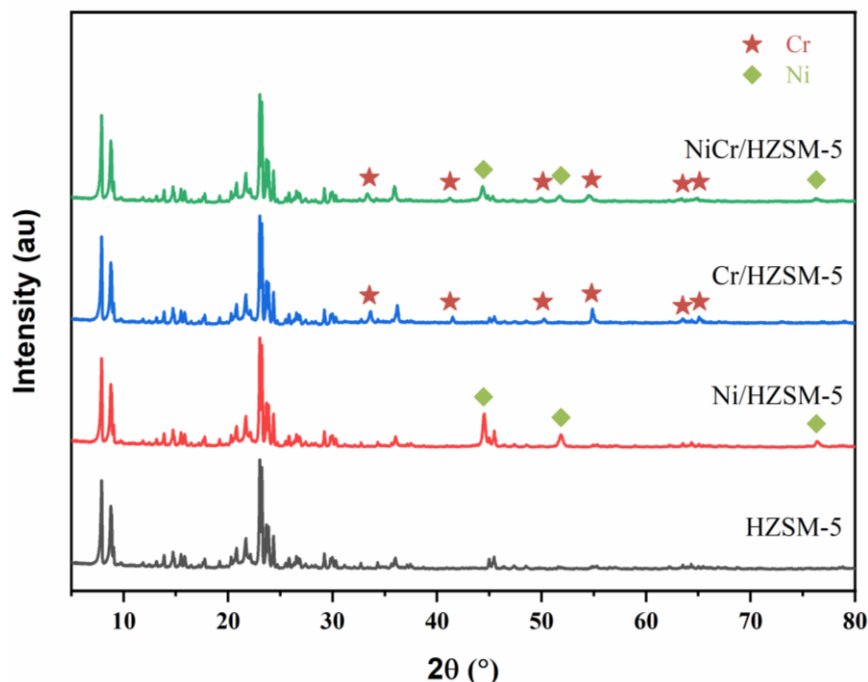


**Fig. 1.** XRD patterns for Cr/HZSM-5, Ni/HZSM-5, and NiCr/HZSM-5 catalysts

To further analyze the constituent elements and chemical state of the catalyst, the nickel and chromium monometallic catalysts and the NiCr/HZSM-5 catalyst were analyzed by XPS, and the binding energy of organic pollution carbon C1s was 284.6 eV as a benchmark for binding energy correction. The results are shown in Fig. 2.

Through scanning the full spectrum of the NiCr/HZSM-5 catalyst, the signal peaks of C 1s, O 1s, Si 2p, Al 2p, Ni 2p, and Cr 2p could be clearly observed, as shown in Fig. 2(a), indicating the presence of Ni and Cr two elements on the surface of NiCr/HZSM-5 catalyst, and Si, Al, and O were the three elements of HZSM-5. These were consistent with the XRD characterization results. Figure 2(b) shows the high-resolution XPS spectrum of Ni 2p, from which it could be seen that the Ni 2p XPS spectra could be fit to five peaks with binding energies of 852.5 eV, 856.2 eV, 861.7 eV, 873.9 eV, and 880.4 eV, indicating that the catalyst contained zero-valent Ni, and Ni<sup>2+</sup> was successfully reduced to Ni during the preparation process. Figure 2(c) is the high-resolution XPS spectrum of Cr 2p, from which it could be seen that the Cr 2p XPS spectra could be fit to two peaks with binding energies of 575.8 eV and 577.0 eV (Yu *et al.* 2020), indicating that the catalyst contained Cr<sub>2</sub>O<sub>3</sub>, which further verified the conclusion of XRD. In comparison, the Cr<sup>3+</sup> peak in the NiCr/HZSM-5 catalyst shifted to the direction of high binding energy, indicating that electrons had been transferred between the two metals, and there was a strong interaction (Lin *et al.* 2021), which might be an important reason for the good effect of nickel-chromium bimetal.

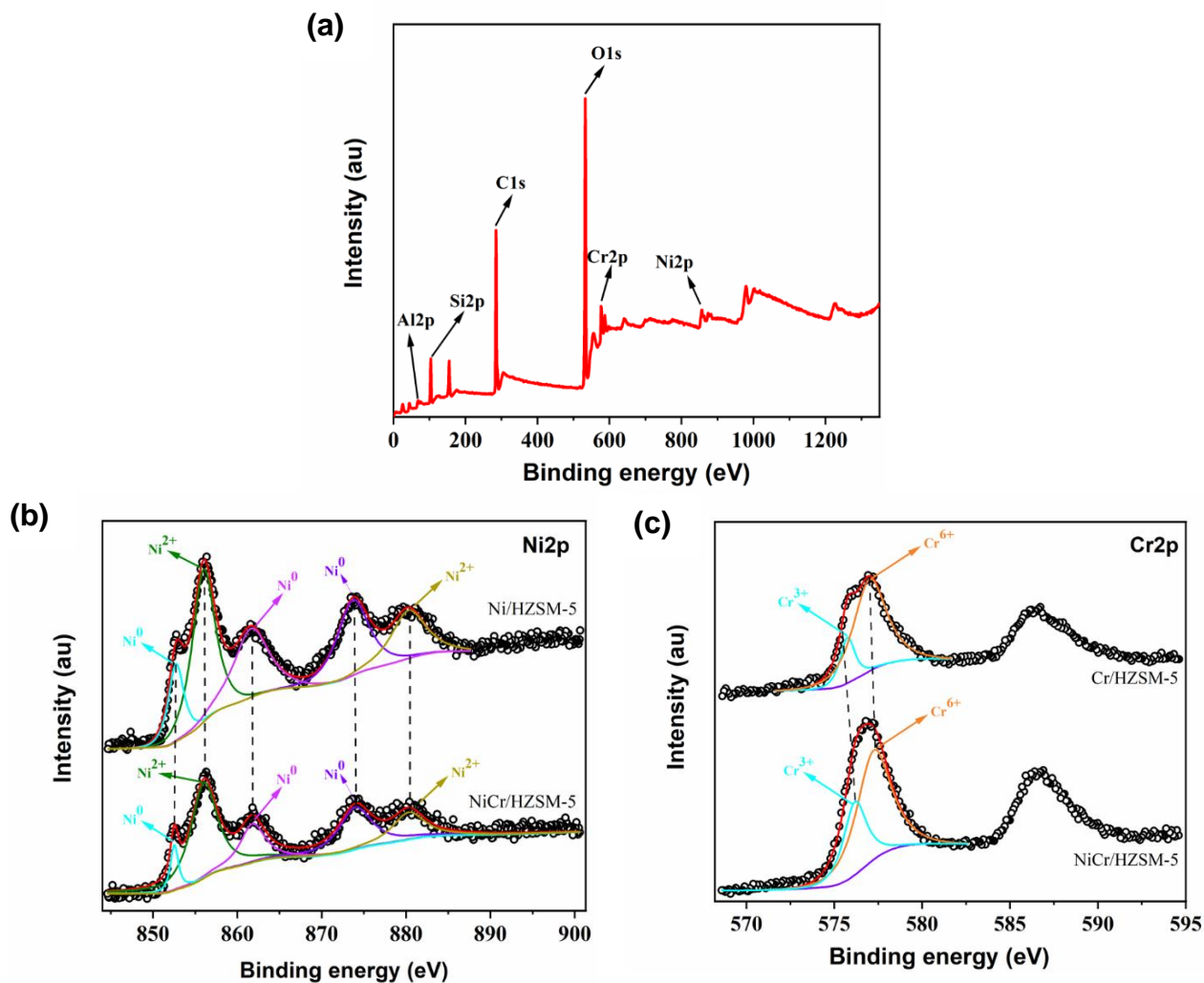


**Fig. 2.** XPS spectrum of NiCr/HZSM-5 catalyst: (a) survey scan of NiCr/HZSM-5 catalyst, (b) high resolution XPS spectrum of Ni 2p, and (c) high resolution XPS spectrum of Cr 2p

The catalysts before and after supporting nickel-chromium bimetal were characterized by nitrogen adsorption-desorption, and the changes of specific surface area and porosity of the catalyst before and after supporting metal were explored, as shown in Fig. 3. From Fig. 3(a), it can be seen that the adsorption-desorption isotherms of HZSM-5 catalyst before and after supporting nickel-chromium bimetal all increased rapidly at a lower relative pressure. After reaching a certain relative pressure, the adsorption saturation value appeared, which was a typical type I isotherm, and the hysteresis ring was H4, indicating that the catalyst had a typical microporous structure.

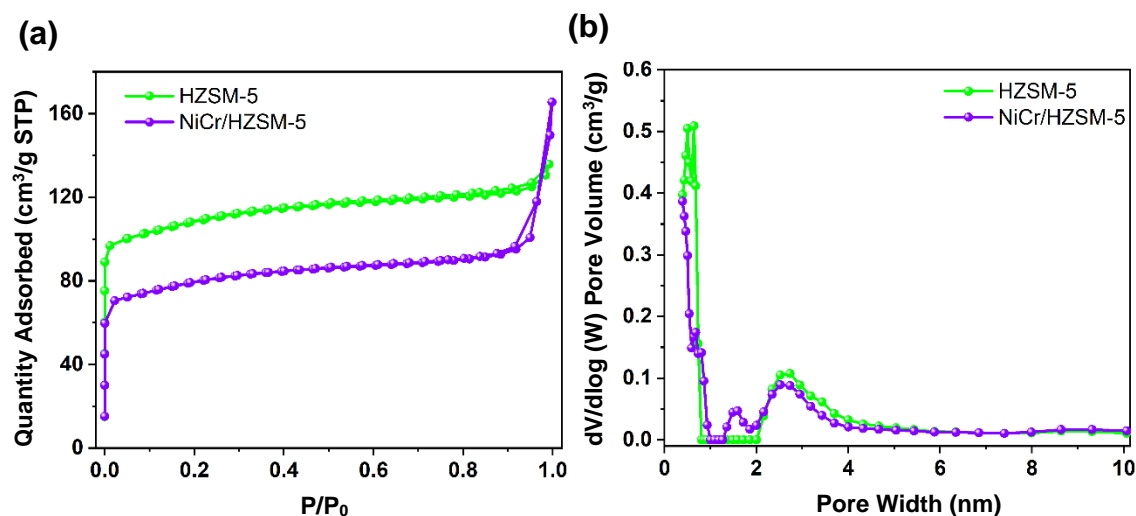


**Fig. 3.** (a) NiCr/HZSM-5 catalyst nitrogen adsorption-desorption isotherm and (b) NiCr/HZSM-5 catalyst pore size distribution

The pore size distribution in Fig. 3(b) showed that the catalyst pore size was mainly distributed within 2 nm, while a small amount of mesopores existed between 2 and 4 nm, which might be due to the formation of catalyst accumulation, indicating that the catalyst was a typical microporous material, consistent with previous studies (Zeng *et al.* 2021). In combination with Table 1, it can be seen that the specific surface area of the catalyst was remarkably reduced after supported nickel and chromium bimetals, especially the specific surface area of the micropores, indicating that most of the metal was supported on the surface of the catalyst micropores, and the pore volume was also reduced, indicating that a small amount of metal was distributed in the pores, further verifying the conclusion of XRD.

**Table 1.** Specific Surface Area and Pore Volume of Catalyst

| Sample      | N <sub>2</sub> Adsorption-desorption           |                    |                  |  |                    |
|-------------|--|--------------------|------------------|--|--------------------|
|             | Surface Area (m <sup>2</sup> g <sup>-1</sup> ) |                    |                  | Pore Volume (cm <sup>3</sup> g <sup>-1</sup> ) |                    |
|             | S <sub>BET</sub>                               | S <sub>micro</sub> | S <sub>ext</sub> | V <sub>total</sub>                             | V <sub>micro</sub> |
| HZSM-5      | 415  | 307                | 107              | 0.19   | 0.12               |
| NiCr/HZSM-5 | 300  | 205                | 94.7             | 0.15   | 0.08               |

S<sub>BET</sub>: Specific surface area calculated by the BET method; S<sub>micro</sub>: Micropore area calculated by the t-Plot method; S<sub>ext</sub>: External surface area calculated by the t-Plot method; V<sub>total</sub>: Single point adsorption total pore volume of pores; and V<sub>micro</sub>: Micropore volume calculated by the t-Plot method

The acidity of the catalyst has an important effect on the reaction (Yu *et al.* 2012). Studies (Kim *et al.* 2015a) have shown that the acidity of the HZSM-5 catalyst is the main factor affecting the yield of depolymerized monomers. The acidity of the catalyst surface was characterized by NH<sub>3</sub>-TPD. The results are shown in Fig. 4.

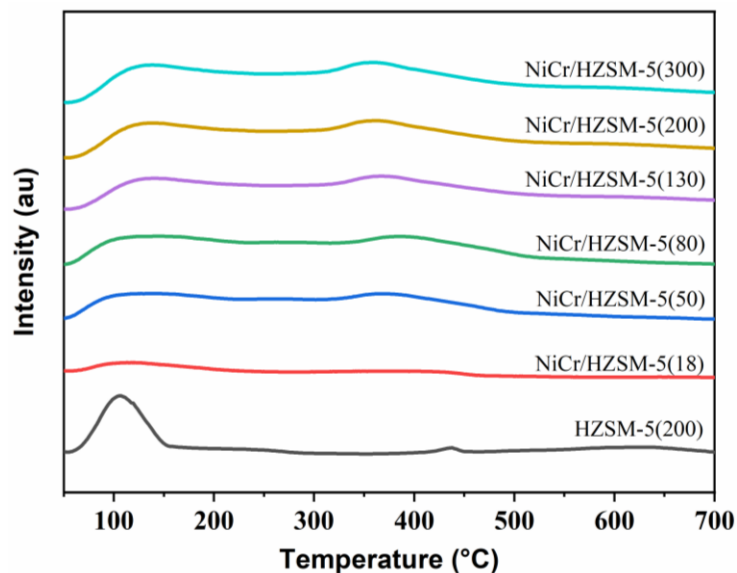


**Fig. 4.** NH<sub>3</sub>-TPD curves of HZSM-5 catalysts with different Si/Al

Supports with different surface acid strengths have different binding energies with ammonia. The desorption temperature range of chemically adsorbed ammonia is used to characterize the surface acid strength of the support. The low temperature desorption peak between 150 and 250 °C belonged to the weak acid center, the middle temperature desorption peak between 250 and 400 °C belonged to the medium strong acid center, and the high temperature desorption peak above 400 °C belonged to the strong acid center (Fang *et al.* 2020). Combined with Table 2, it could be seen that HZSM-5 supported with nickel-chromium bimetal generally had medium and strong acid centers, while HZSM-5 without metal loading only had a small number of weak acid centers and strong acid centers. The strong acid centers and weak acid centers of HZSM-5 catalysts supported with nickel-chromium bimetal were remarkably increased, and the increase of acidity might be one of the reasons for the increased activity of catalyst for lignin liquefaction depolymerization. As shown by (Mihalcik *et al.* 2011), the acidity of the HZSM-5 decreases with the increase of the Si/Al, while the acidity of the catalyst supported with nickel-chromium bimetal increased with the increase of the Si/Al of the support. This might be because the surface acidity of HZSM-5 was remarkably increased after preparation of the supported nickel-chromium bimetal.

**Table 2.** Acidity of HZSM-5 Supported Catalysts with Different Si/Al

| Catalyst         | Weak Acidity (μmol/g) | Medium Strong Acidity (μmol/g) |
|------------------|-----------------------|--------------------------------|
| HZSM-5(200)      | 15.73                 | 10.32                          |
| NiCr/HZSM-5(18)  | 57.72                 | 24.30                          |
| NiCr/HZSM-5(50)  | 43.40                 | 20.24                          |
| NiCr/HZSM-5(80)  | 47.20                 | 21.35                          |
| NiCr/HZSM-5(130) | 50.05                 | 22.87                          |
| NiCr/HZSM-5(200) | 53.00                 | 23.49                          |
| NiCr/HZSM-5(300) | 55.00                 | 24.21                          |

## Catalytic Liquefaction of EOL Into Bio-oil and Monophenol

Different metals have different catalytic activities relative to the depolymerization of lignin, and transition metals have been reported to have good catalytic activity and are more economical than precious metals (Ye *et al.* 2021). It can be seen from Fig. 5 that active metals have an important effect on the catalytic depolymerization of lignin.

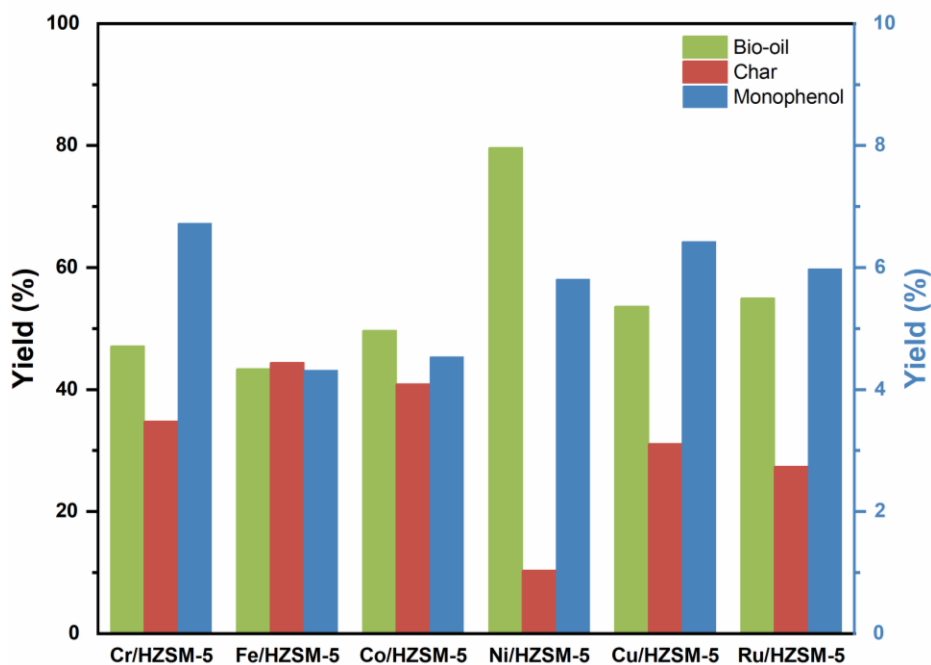


**Fig. 5.** Catalytic liquefaction of EOL over different catalysts. Reaction conditions: 0.50 g lignin, 0.10 g catalyst, 10% catalyst metal loading, Si/Al = 50, 12 g ethanol, 280 °C, 2 h, and 500 rpm (Blue bars are related to y2 while the other ones to y1, the following are the same.)

Among them, the bio-oil yield of nickel-based catalysts was as high as 79.6%, and the amount of char was the least, which was 10.3%. This might be due to the high hydrogenation activity of nickel ( Song *et al.* 2013; Sridhar *et al.* 2020; Lin *et al.* 2021), which could effectively increase the yield of bio-oil and inhibit the formation of char. The chromium-based catalyst had the highest monophenol yield. This might be because the Cr species supported on HZSM-5 zeolite had higher catalytic activity, but its bio-oil yield was low and there was more char. This might be related to its low hydrogenation activity and certain oxidizing properties (Yu *et al.* 2020). However, iron and cobalt have low activity as single metal catalysts, low liquefaction rate of lignin and more char, generally combined with other active metals to form bimetallic catalysts with higher catalytic activity (Kim *et al.* 2015c; Zhai *et al.* 2017; Dou *et al.* 2020; Lu *et al.* 2020; Mauriello *et al.* 2020). The char of copper-based catalysts was less than that of Fe, Co, and Cr single-metal catalysts, probably because copper could reduce char formation (Barta *et al.* 2014), but its hydrogenation activity was not as good as nickel-based catalysts.

The Cr/HZSM-5 monometallic catalyst had a higher monophenol yield, but a lower lignin liquefaction rate and more char. Therefore, Cr was compounded with the other four transition metals, Fe, Co, Ni, and Cu, and the noble metal Ru to explore the depolymerization effect of the chromium-based bimetallic catalyst, as shown in Fig. 6. Through comparison, it was found that the yield of chromium-based bimetallic catalysts

was slightly higher than that of monometallic catalysts. This might be because the interaction between the two metals changed the electronic structure of the catalyst surface, thereby increasing its catalytic activity (Gao *et al.* 2019; Kong *et al.* 2020), while the bio-oil yields of Ni-Cr and Ru-Cr bimetallic catalysts both reached more than 90%, and there was no obvious char. This showed that Cr had a good synergistic effect with Ni and Ru respectively, which could promote the liquefaction of lignin and reduce the production of char. However, ruthenium, as a precious metal, was not economical, so the NiCr/HZSM-5 bimetallic catalyst was used as the optimal catalyst to further explore.

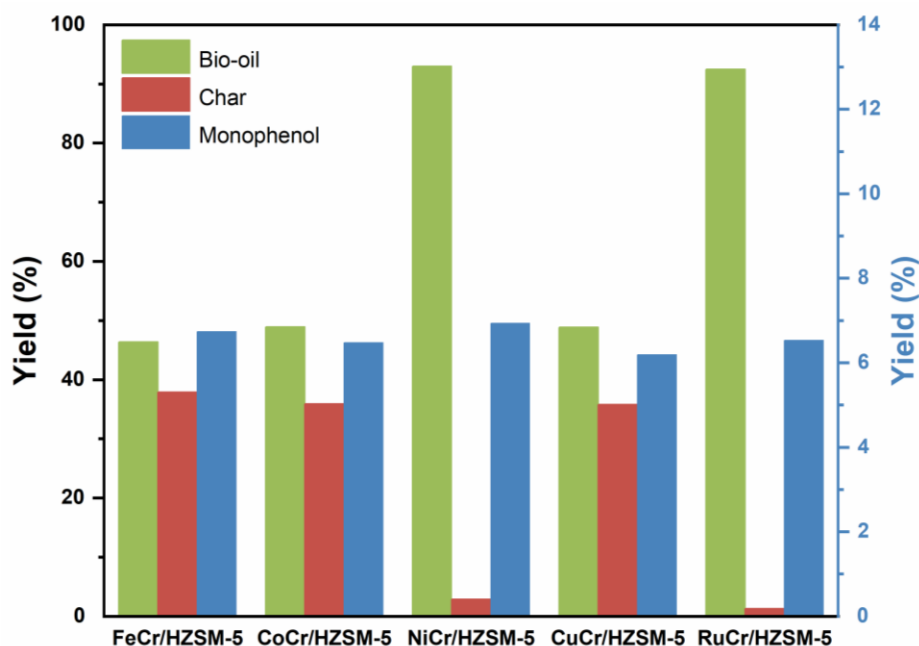


**Fig. 6.** Different chromium-based bimetallic catalysts; reaction conditions: 0.50 g lignin, 0.10 g catalyst, 10% catalyst metal loading (each), Si/Al = 50, 12 g ethanol, 280 °C, 2 h, and 500 rpm

Therefore, the NiCr/HZSM-5 bimetallic catalyst was used as the optimal catalyst to further explore the effect of loading (Fig. 7). The results showed that as the overall metal loading increased, the lignin liquefaction rate gradually increased, and the char rate decreased, but the monophenol yield did not change noticeably. It might be that the increase of metal sites was conducive to the liquefaction of lignin and the reduction of char production, and the monophenol yield reached the highest at 6.94% when the ratio of nickel to chromium was 10:10.

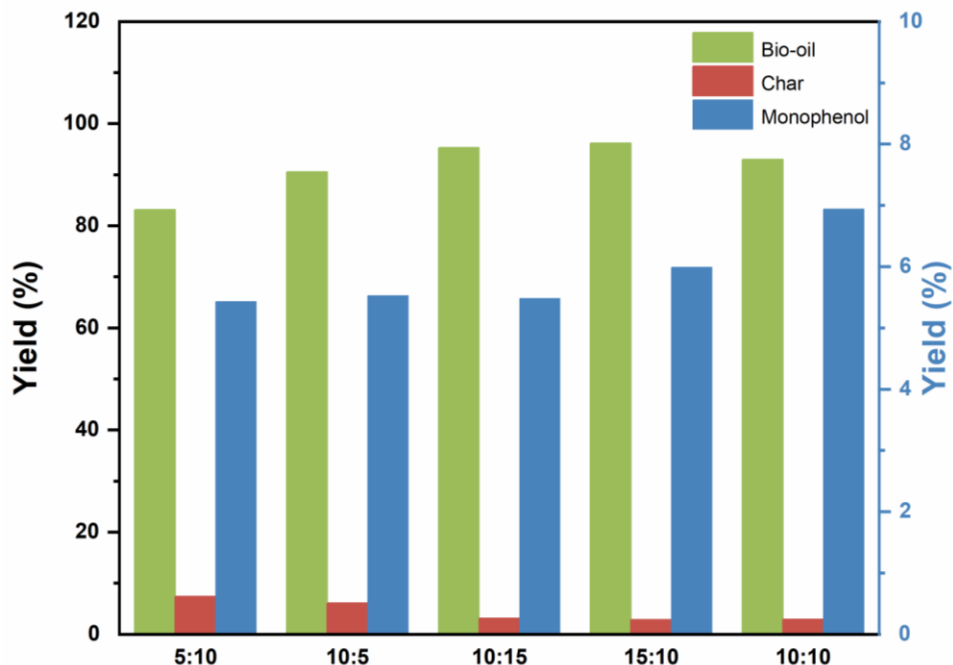


**Fig. 7.** Catalysts with different ratios of nickel to chromium; reaction conditions: 0.50 g lignin, 0.10 g catalyst, 10% catalyst metal loading (each), Si/Al = 50, 12 g ethanol, 280 °C, 2 h, and 500 rpm

### The Effect of Catalyst Support

Previous studies (Singh and Ekhe 2014b; Gardner *et al.* 2015; Jan *et al.* 2015) have shown that the silica-alumina ratio of HZSM-5 zeolite had a significant effect on its catalytic performance. To investigate the effect of different Si/Al of the support on the depolymerization activity of lignin, a series of nickel-chromium bimetallic catalyst supported on different silicon-to-aluminum ratios were prepared and explored (Fig. 8). With the increase in the ratio of silicon to aluminum, both the liquefaction rate of lignin and the yield of monophenols increased slightly, and the amount of char did not change noticeably. When the ratio of silica to aluminum in the zeolite carrier was 200, the liquefaction percent of lignin was 96.0%, and the yield of monophenols reached 7.87%. This might be because the different ratios of silicon to aluminum of the support lead to differences in the acidity of the catalyst (Aho *et al.* 2008; Shirazi *et al.* 2008). Proper acidity of the catalyst could promote the cleavage of the  $\beta$ -O-4 and  $\alpha$ -O-4 ether bonds, whereas excessive acidity could cause the recondensation of active monomers and increase the amount of char (Chen *et al.* 2017). At the same time, previous studies (Ben and Ragauskas 2013) have shown that HZSM-5 with higher Si/Al was beneficial to degrade aromatic C-C bonds and prevented the recondensation of lignin depolymerization products, which is consistent with the conclusions of the current study (Kim *et al.* 2015a).

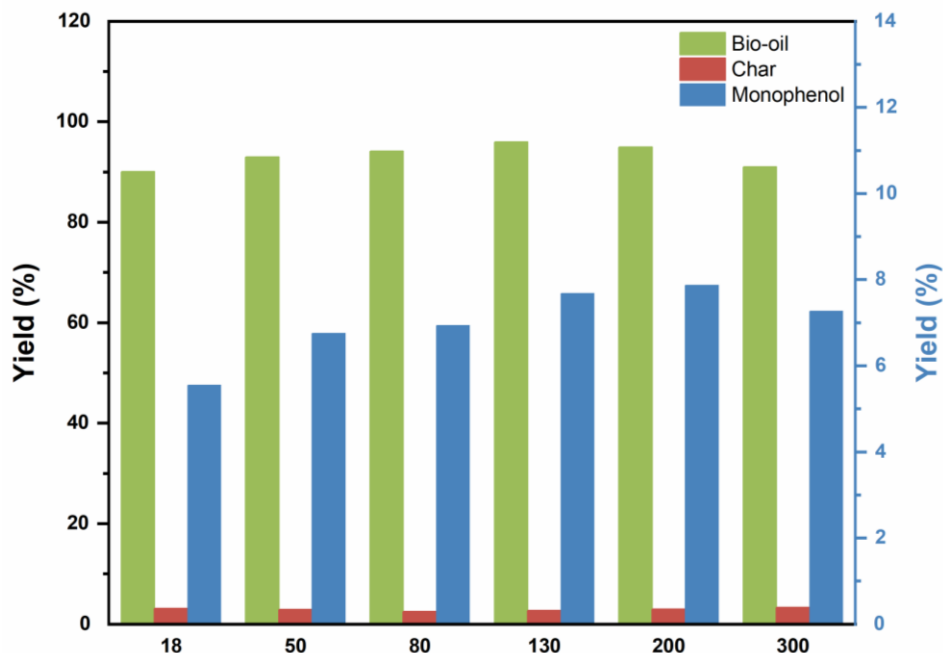


**Fig. 8.** Catalysts with different ratios of silicon to aluminium; reaction conditions: 0.50 g lignin, 0.10 g catalyst, 10% catalyst metal loading (each), 12 g ethanol, 280 °C, 2 h, and 500 rpm

As shown in Fig. 9, the authors compared NiCr/HZSM-5 (200) with commercial Raney Ni catalyst and found that no matter the addition of zeolite supported nickel-chromium bimetallic catalyst or Raney Ni catalyst, the liquefaction rate of lignin was remarkably increased, the monophenol production rate was also increased to a certain extent, and the amount of char was remarkably reduced.

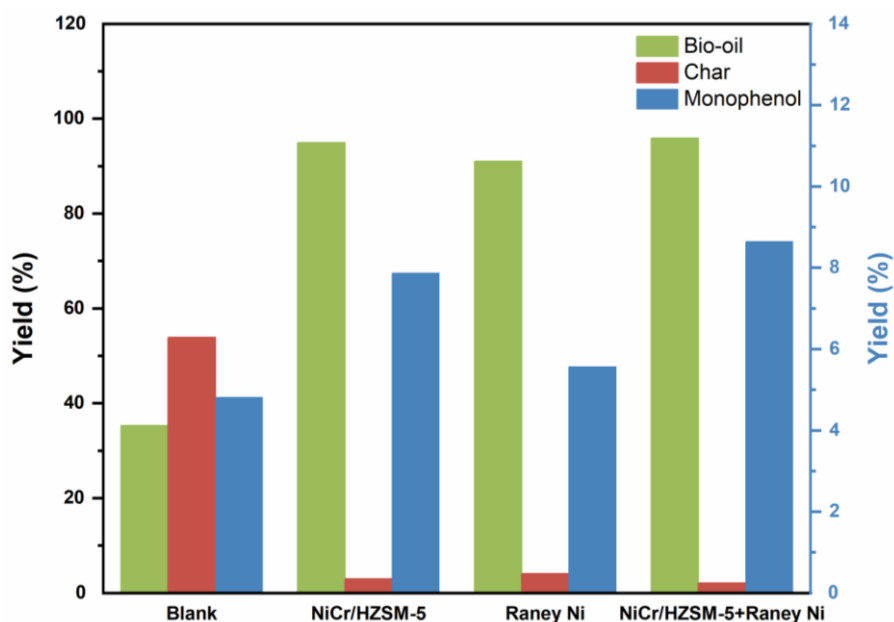
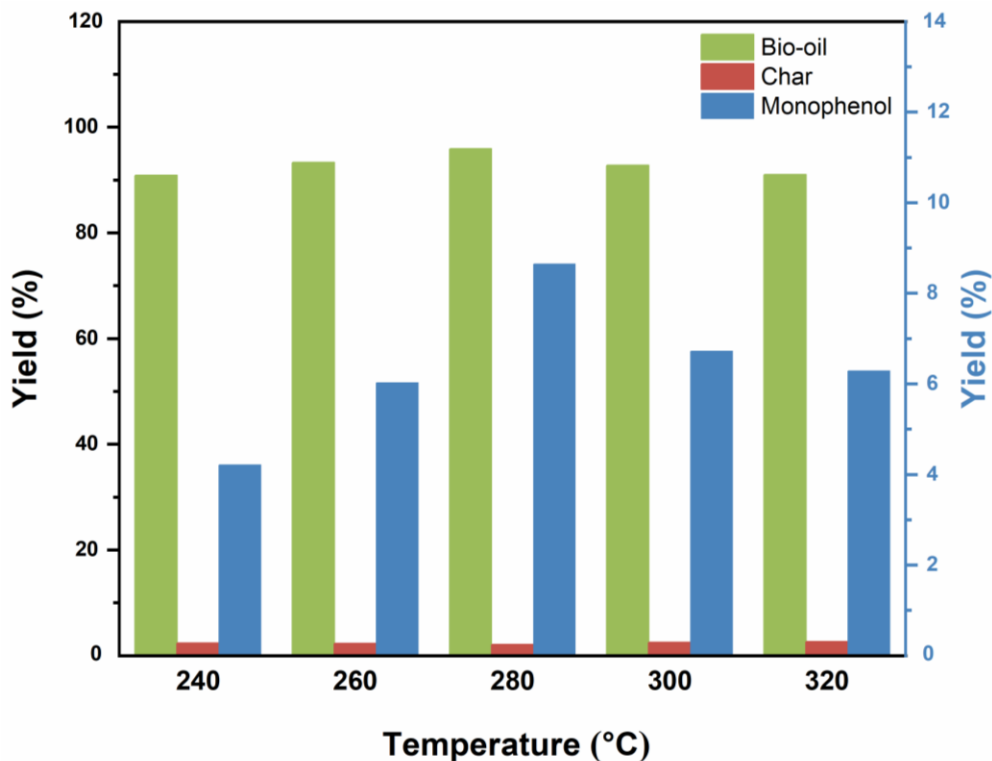


**Fig. 9.** Effect comparison with Raney Ni catalyst; reaction conditions: 0.50 g lignin, 0.10 g catalyst (each), 10% catalyst metal loading (each), Si/Al = 200, 12 g ethanol, 280 °C, 2 h, and 500 rpm

Furthermore, the NiCr/HZSM-5 (200) catalyst had better catalytic effect than commercial Raney Ni catalyst. It achieved higher lignin liquefaction rate and lower char content. When the zeolite supported nickel-chromium bimetallic catalyst and Raney Ni catalyst were added at the same time, the liquefaction rate, char rate, and monophenol yield of lignin reached extreme values. The highest liquefaction rate was 95.90%, the highest monophenol yield was 8.64%, and the char amount was 2.08%, indicating that the zeolite supported nickel-chromium bimetallic catalyst and Raney Ni catalyst had a certain synergistic effect.

### The Effect of Reaction Temperature and Time

Because the reaction temperature and time have a certain effect on the depolymerization of lignin, the differences in the depolymerization effects of lignin at different temperatures and times were respectively explored, as shown in Fig. 10. With the increase of temperature, the liquefaction rate of lignin and the yield of monophenols both increased, reaching the highest value at 280 °C, and gradually decreasing with the increase of temperature after 280 °C. This might be because the temperature was too high, which would aggravate the recondensation reaction of the depolymerization products, thus leading to a decrease in the yield of bio-oil and monophenols (Shu *et al.* 2016b). As the reaction time increased, the yields of bio-oil and monophenols increased first and then decreased, while the amount of char slightly increased. This might be that due to the prolongation of the reaction time, the lignin was fully depolymerized, while the condensation reaction was still proceeding (Chen *et al.* 2017). If the reaction time was too long, the depolymerized product would have slight recondensation (Lin *et al.* 2021).



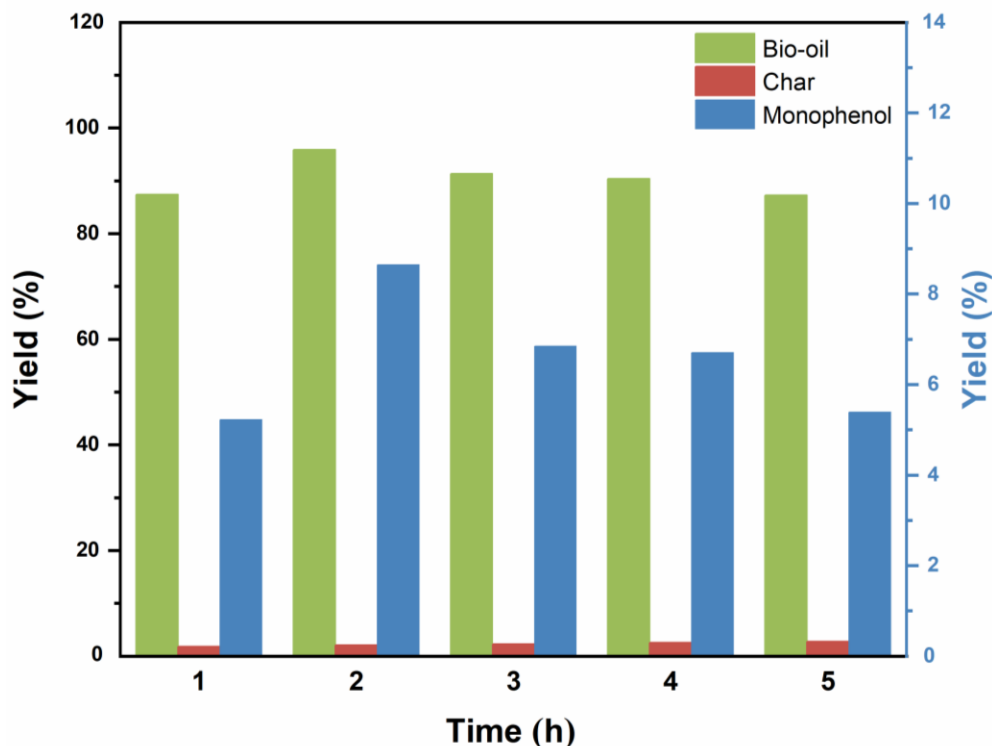


**Fig. 10.** The effect of reaction temperature and time; reaction conditions: 0.50 g lignin, 0.10 g catalyst (each), 10% catalyst metal loading (each), Si/Al = 200, 12 g ethanol, and 500 rpm

### Analysis of Depolymerization Products

The identification and analysis of lignin liquefaction products was obtained by GC-MS. It could be seen from Fig. 11 that the liquefied product was mainly composed of alkylphenol compounds. The substituents of phenolic compounds included alkyl, hydroxyl, methoxy, *etc.*, and these alkylphenol compounds were typical lignin structural units, indicating that lignin successfully depolymerized into small molecular monomers.

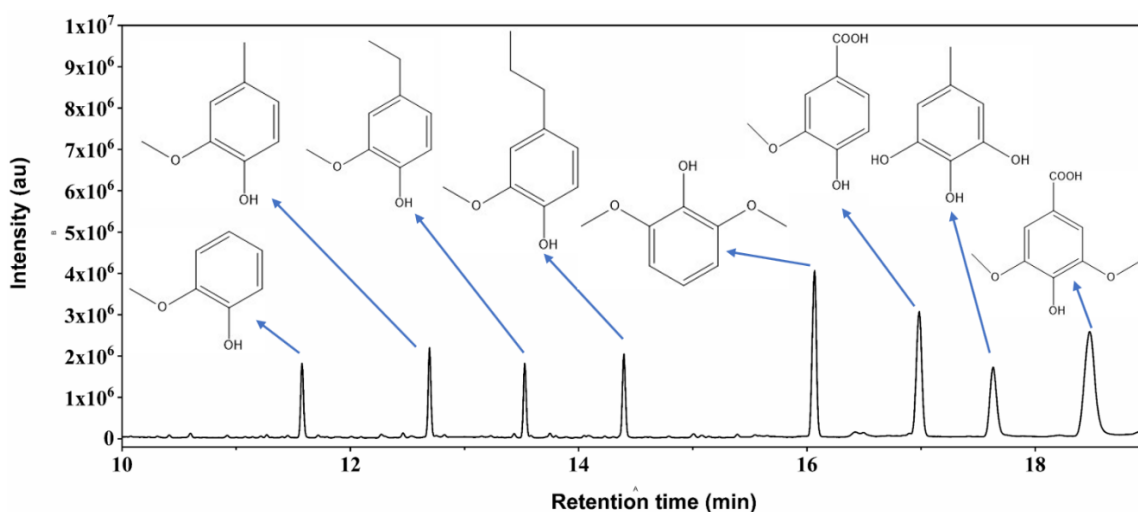


**Fig. 11.** GC-MS analysis of liquid products; reaction conditions: 0.50 g lignin, 0.10 g NiCr/HZSM-5(200), 12 g ethanol, 280 °C, 2 h, and 500 rpm

Fourier transform infrared spectroscopy was used to characterize the raw EOL and the lignin oil (LO) produced under the optimal process conditions. The results are shown in Fig. 12. It can be seen that the lignin had a similar functional group structure before and after liquefaction. The peaks appearing at 3434 and 2930  $\text{cm}^{-1}$  were attributed to the stretching of  $-\text{OH}$  and  $-\text{OCH}_3$ , respectively, while the peaks appearing at 1704  $\text{cm}^{-1}$  were attributed to the  $\text{C}=\text{O}$  stretching vibration (Chen *et al.* 2020). The peaks appearing at 1605, 1513, 1449, and 829  $\text{cm}^{-1}$  were the vibration of the aromatic ring in lignin (Fushimi *et al.* 2009), indicating that the lignin had a typical phenolic or ether aromatic monomer structure before and after depolymerization, which was consistent with the results of GC-MS. The peaks appearing at 1265, 1219, 1141, 1097, and 1050  $\text{cm}^{-1}$  in the FTIR spectrum of EOL were attributed to the Ar-O stretching breathing (Long *et al.* 2014); the disappearance or weakening of these peaks in the LO spectrum indicated that the lignin aromatic ether bonds were broken, and further indicated that NiCr/HZSM-5 could effectively catalyze the depolymerization of EOL. The peaks appearing at 1325  $\text{cm}^{-1}$  in the FTIR spectrum of EOL were attributed to the C5 vibration on condensed S or G ring (Chen *et al.* 2020), and the disappearance in the LO spectrum indicated the effective fracture of C5 on condensed S or G ring.

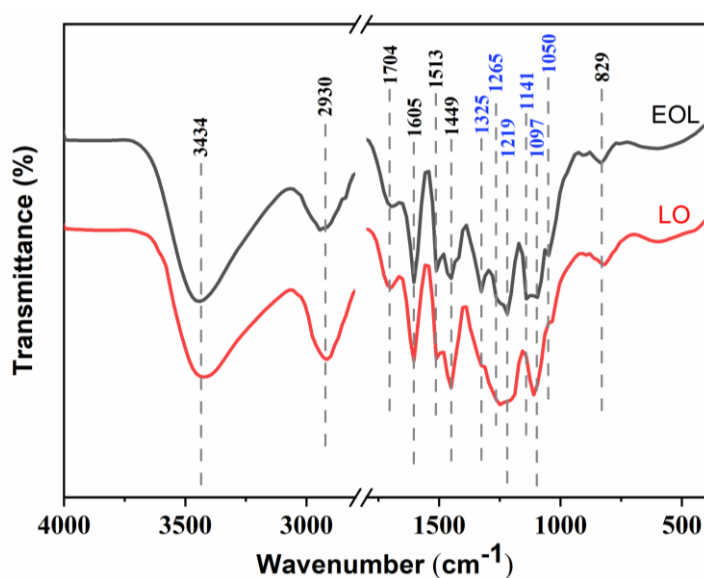


**Fig. 12.** FTIR spectra of EOL and LO; reaction conditions: 0.50 g lignin, 0.10 g NiCr/H-ZSM-5 + 0.10 g Raney Ni, 12 g ethanol, 280 °C, 2 h, and 500 rpm

The lignin before and after depolymerization was characterized by  $^1\text{H}$ - $^{13}\text{C}$  HSQC NMR, as shown in Fig. 13. From Figs. 13(a) and (b) of the benzene ring area, it could be seen that there were three types of monomers: G, S, and H in raw EOL, which were consistent with the characteristics of hardwood, while there were only two types of monomers, S and G, in LO after depolymerization, indicating that the product contained a large number of S-type monomers, which was consistent with the GC-MS detection results. From Fig. 13(c), it could be seen that EOL was rich in  $\beta$ -5 and  $\beta$ - $\beta$  linkages, and had a large number of methoxy groups (Lei *et al.* 2019), which were typical linkages between lignin structural units.

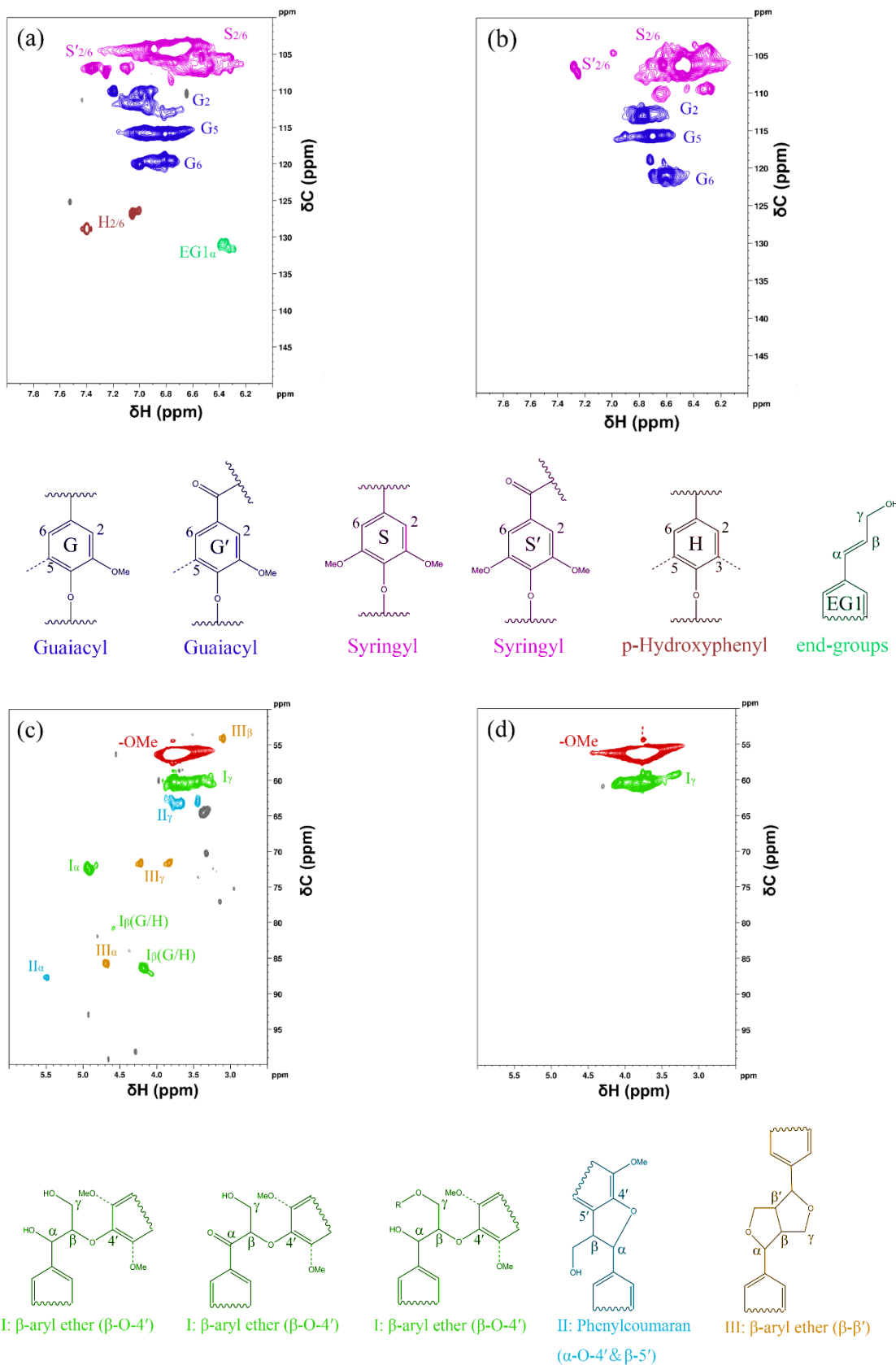


**Fig. 13.**  $^1\text{H}$ - $^{13}\text{C}$  HSQC NMR spectra of EOL (a, c) and LO (b, d); reaction conditions: 0.50 g lignin, 0.10 g NiCr/H-ZSM-5 + 0.10 g Raney Ni, 12 g ethanol, 280  $^{\circ}\text{C}$ , 2 h, and 500 rpm

Comparing Fig. 13(d), it could be found that only the methoxy group and  $\beta$ -O-4 linkage signal remained after the catalytic depolymerization. This might be because lignin had more than 50%  $\beta$ -O-4 linkages (Zakzeski *et al.* 2010), and there were still a small amount of residual ether linkages after depolymerization, while the  $\beta$ -5 and  $\beta$ - $\beta$  linkage signals of lignin disappeared, indicating that EOL was effectively depolymerized into oligomers and monomers, consistent with the detection results of FTIR and GC-MS.

## CONCLUSIONS

1. The NiCr/HZSM-5 catalyst could efficiently catalyze the liquefaction of eucalyptus organosolv lignin (EOL), and the catalytic effect was better than Ru-based precious metal catalysts and commercial Raney Ni catalysts. The Ni and Cr metals had a good synergistic effect.
2. After HZSM-5 was supported with nickel-chromium bimetal, the acidity of the catalyst was remarkably enhanced, which was beneficial to the catalytic cracking of lignin.
3. The optimized process conditions were as follows: NiCr/HZSM-5(200) and Raney Ni synergistically catalyzed the reaction in ethanol system at 280 °C for 2 h, the liquefaction rate of EOL reached 95.90%, the monophenol yield was 8.64%, and the char content was only 2.08%. Additionally, the yield of lignin oil was remarkably higher than the 83% lignin oil yield obtained by pretreating lignin with hydrogen peroxide (Qi *et al.* 2017) and the 77.4% lignin oil yield obtained with precious metal-based catalysts reported in the literature (Kim *et al.* 2015b).
4. NiCr/HZSM-5 catalyst has lower cost and higher activity than noble metal-based catalysts and commercial Raney Ni, which is a promising catalyst for lignin valorization.

## ACKNOWLEDGMENTS

This work was supported by the National Natural Science Foundation of China (Grant No. 31870558); the Science and Technology Project of Guangzhou City (Grant No. 202002030157); Key Research and Development Program of Shandong Province (Grant No. 2019JZZY010501); and the Guangdong Basic and Applied Basic Research Foundation (Grant No. 2021A1515012364).

## REFERENCES CITED

- Aho, A., Kumar, N., Eränen, K., Salmi, T., Hupa, M., and Murzin, D.Y. (2008). "Catalytic pyrolysis of woody biomass in a fluidized bed reactor: Influence of the zeolite structure," *Fuel* 87(12), 2493-2501. DOI: 10.1016/j.fuel.2008.02.015
- Barta, K., Warner, G. R., Beach, E. S., and Anastas, P. T. (2014). "Depolymerization of organosolv lignin to aromatic compounds over Cu-doped porous metal oxides," *Green Chemistry* 16(1), 191-196. DOI: 10.1039/C3GC41184B

- Ben, H., and Ragauskas, A. J. (2013). "Influence of Si/Al ratio of ZSM-5 zeolite on the properties of lignin pyrolysis products," *ACS Sustainable Chemistry & Engineering* 1(3), 316-324. DOI: 10.1021/sc300074n
- Chen, P., Zhang, Q., Shu, R., Xu, Y., Ma, L., and Wang, T. (2017). "Catalytic depolymerization of the hydrolyzed lignin over mesoporous catalysts," *Bioresource Technology* 226, 125-131. DOI: 10.1016/j.biortech.2016.12.030
- Chen, S., Cheng, H., and Wu, S. (2020). "Pyrolysis characteristics and volatiles formation rule of organic solvent fractionized kraft lignin," *Fuel* 270, article no. 117520. DOI: 10.1016/j.fuel.2020.117520
- Deuss, P. J., Lancefield, C. S., Narani, A., de Vries, J. G., Westwood, N. J., Barta, K. (2017). "Phenolic acetals from lignins of varying compositions via iron(iii) triflate catalysed depolymerisation," *Green Chemistry* 19(12), 2774-2782. DOI: 10.1039/C7GC00195A
- Dou, X., Jiang, X., Li, W., Zhu, C., Liu, Q., Lu, Q., Zheng, X., Chang, H.-m., and Jameel, H. (2020). "Highly efficient conversion of kraft lignin into liquid fuels with a Co-Zn-beta zeolite catalyst," *Applied Catalysis B: Environmental* 268, article no. 118429. DOI: 10.1016/j.apcatb.2019.118429
- Fang, Q., Jiang, Z., Guo, K., Liu, X., Li, Z., Li, G., and Hu, C. (2020). "Low temperature catalytic conversion of oligomers derived from lignin in pubescens on Pd/NbOPO<sub>4</sub>," *Applied Catalysis B: Environmental* 263, article no. 118325. DOI: 10.1016/j.apcatb.2019.118325
- Fushimi, C., Katayama, S., Tasaka, K., Suzuki, M., and Tsutsumi, A. (2009). "Elucidation of the interaction among cellulose, xylan, and lignin in steam gasification of woody biomass," *AIChE Journal* 55(2), 529-537. DOI: 10.1002/aic.11705
- Galkin, M. V., and Samec, J. S. M. (2016). "Lignin valorization through catalytic lignocellulose fractionation: A fundamental platform for the future biorefinery," *ChemSusChem* 9(13), 1544-1558. DOI: 10.1002/cssc.201600237
- Gao, X., Zhu, S., and Li, Y. (2019). "Selective hydrogenolysis of lignin and model compounds to monophenols over AuPd/CeO<sub>2</sub>," *Molecular Catalysis* 462, 69-76. DOI: 10.1016/j.mcat.2018.10.022
- Gardner, D. W., Huo, J., Hoff, T. C., Johnson, R. L., Shanks, B. H., and Tessonier, J.-P. (2015). "Insights into the hydrothermal stability of ZSM-5 under relevant biomass conversion reaction conditions," *ACS Catalysis* 5(7), 4418-4422. DOI: 10.1021/acscatal.5b00888
- Gaspar, A. B., Perez, C. A. C., and Dieguez, L. C. (2005). "Characterization of Cr/SiO<sub>2</sub> catalysts and ethylene polymerization by XPS," *Applied Surface Science* 252(4), 939-949. DOI: 10.1016/j.apsusc.2005.01.031
- Jan, O., Marchand, R., Anjos, L. C. A., Seufitelli, G. V. S., Nikolla, E., and Resende, F. L. P. (2015). "Hydropyrolysis of lignin using Pd/HZSM-5," *Energy & Fuels* 29(3), 1793-1800. DOI: 10.1021/ef502779s
- Kim, J.-Y., Lee, J. H., Park, J., Kim, J. K., An, D., Song, I. K., and Choi, J. W. (2015a). "Catalytic pyrolysis of lignin over HZSM-5 catalysts: Effect of various parameters on the production of aromatic hydrocarbon," *Journal of Analytical and Applied Pyrolysis* 114, 273-280. DOI: 10.1016/j.jaap.2015.06.007
- Kim, J.-Y., Park, J., Kim, U.-J., and Choi, J. W. (2015b). "Conversion of lignin to phenol-rich oil fraction under supercritical alcohols in the presence of metal catalysts," *Energy & Fuels* 29(8), 5154-5163. DOI: 10.1021/acs.energyfuels.5b01055

- Kim, J. K., Lee, J. K., Kang, K. H., Song, J. C., and Song, I. K. (2015c). "Selective cleavage of CO bond in benzyl phenyl ether to aromatics over Pd–Fe bimetallic catalyst supported on ordered mesoporous carbon," *Applied Catalysis A: General*, 498, 142-149. DOI: 10.1016/j.apcata.2015.03.034
- Kong, L., Liu, C., Gao, J., Wang, Y., and Dai, L. (2019). "Efficient and controllable alcoholysis of kraft lignin catalyzed by porous zeolite-supported nickel-copper catalyst," *Bioresource Technology* 276, 310-317. DOI: 10.1016/j.biortech.2019.01.015
- Kong, L., Zhang, L., Gu, J., Gou, L., Xie, L., Wang, Y., and Dai, L. (2020). "Catalytic hydrotreatment of kraft lignin into aromatic alcohols over nickel-rhenium supported on niobium oxide catalyst," *Bioresource Technology* 299, article no. 122582. DOI: 10.1016/j.biortech.2019.122582
- Lei, M., Wu, S., Liang, J., and Liu, C. (2019). "Comprehensive understanding the chemical structure evolution and crucial intermediate radical in situ observation in enzymatic hydrolysis/mild acidolysis lignin pyrolysis," *Journal of Analytical and Applied Pyrolysis* 138, 249-260. DOI: 10.1016/j.jaap.2019.01.004
- Lin, F., Ma, Y., Sun, Y., Zhao, K., Gao, T., and Zhu, Y. (2021). "Heterogeneous Ni–Ru/H-ZSM-5 one-pot catalytic conversion of lignin into monophenols," *Renewable Energy* 170, 1070-1080. DOI: 10.1016/j.renene.2021.01.150
- Long, J., Zhang, Q., Wang, T., Zhang, X., Xu, Y., and Ma, L. (2014). "An efficient and economical process for lignin depolymerization in biomass-derived solvent tetrahydrofuran," *Bioresource Technology* 154, 10-17. DOI: 10.1016/j.biortech.2013.12.020
- Lu, X., Zhu, X., Guo, H., Que, H., Wang, D., Liang, D., He, T., Hu, C., Xu, C., and Gu, X. (2020). "Efficient depolymerization of alkaline lignin to phenolic compounds at low temperatures with formic acid over inexpensive Fe–Zn/Al<sub>2</sub>O<sub>3</sub> catalyst," *Energy & Fuels* 34(6), 7121-7130. DOI: 10.1021/acs.energyfuels.0c00742
- Mauriello, F., Ariga-Miwa, H., Paone, E., Pietropaolo, R., Takakusagi, S., and Asakura, K. (2020). "Transfer hydrogenolysis of aromatic ethers promoted by the bimetallic Pd/Co catalyst," *Catalysis Today* 357, 511-517. DOI: 10.1016/j.cattod.2019.06.071
- Mihalcik, D. J., Mullen, C. A., and Boateng, A. A. (2011). "Screening acidic zeolites for catalytic fast pyrolysis of biomass and its components," *Journal of Analytical and Applied Pyrolysis* 92(1), 224-232. DOI: 10.1016/j.jaap.2011.06.001
- Patil, V., Adhikari, S., Cross, P., and Jahromi, H. (2020). "Progress in the solvent depolymerization of lignin," *Renewable and Sustainable Energy Reviews* 133, article no. 110359. DOI: 10.1016/j.rser.2020.110359
- Qi, S.-C., Hayashi, J.-i., Kudo, S., and Zhang, L. (2017). "Catalytic hydrogenolysis of kraft lignin to monomers at high yield in alkaline water," *Green Chemistry* 19(11), 2636-2645. DOI: 10.1039/C7GC01121K
- Rinaldi, R., Jastrzebski, R., Clough, M. T., Ralph, J., Kennema, M., Bruijninx, P. C. A., and Weckhuysen, B. M. (2016). "Paving the way for lignin valorisation: Recent advances in bioengineering, biorefining and catalysis," *Angewandte Chemie International Edition* 55(29), 8164-8215. DOI: 10.1002/anie.201510351
- Santhosh Kumar, M., Hammer, N., Rønning, M., Holmen, A., Chen, D., Walmsley, J. C., and Øye, G. (2009). "The nature of active chromium species in Cr-catalysts for dehydrogenation of propane: New insights by a comprehensive spectroscopic study," *Journal of Catalysis* 261(1), 116-128. DOI: 10.1016/j.jcat.2008.11.014

- Shao, Y., Xia, Q., Dong, L., Liu, X., Han, X., Parker, S. F., Cheng, Y., Daemen, L. L., Ramirez-Cuesta, A. J., Yang, S., and Wang, Y. (2017). "Selective production of arenes via direct lignin upgrading over a niobium-based catalyst," *Nature Communications* 8(1), article no. 16104. DOI: 10.1038/ncomms16104
- Shirazi, L., Jamshidi, E., and Ghasemi, M. R. (2008). "The effect of Si/Al ratio of ZSM-5 zeolite on its morphology, acidity and crystal size," *Crystal Research and Technology* 43(12), 1300-1306. DOI: 10.1002/crat.200800149
- Shu, R., Long, J., Xu, Y., Ma, L., Zhang, Q., Wang, T., Wang, C., Yuan, Z., and Wu, Q. (2016a). "Investigation on the structural effect of lignin during the hydrogenolysis process," *Bioresource Technology* 200, 14-22. DOI: 10.1016/j.biortech.2015.09.112
- Shu, R., Zhang, Q., Ma, L., Xu, Y., Chen, P., Wang, C., and Wang, T. (2016b). "Insight into the solvent, temperature and time effects on the hydrogenolysis of hydrolyzed lignin," *Bioresource Technology* 221, 568-575. DOI: 10.1016/j.biortech.2016.09.043
- Singh, S. K., and Ekhe, J. D. (2014a). "Solvent effect on HZSM-5 catalyzed solvolytic depolymerization of industrial waste lignin to phenols: superiority of the water-methanol system over methanol," *RSC Advances* 4(95), 53220-53228. DOI: 10.1039/C4RA10240A
- Singh, S. K., and Ekhe, J. D. (2014b). "Towards effective lignin conversion: HZSM-5 catalyzed one-pot solvolytic depolymerization/hydrodeoxygenation of lignin into value added compounds," *RSC Advances* 4(53), 27971-27978. DOI: 10.1039/c4ra02968b
- Song, Q., Wang, F., Cai, J., Wang, Y., Zhang, J., Yu, W., and Xu, J. (2013). "Lignin depolymerization (LDP) in alcohol over nickel-based catalysts via a fragmentation-hydrogenolysis process," *Energy & Environmental Science* 6(3), 994-1007. DOI: 10.1039/c2ee23741e
- Sridhar, A., Rahman, M., Infantes-Molina, A., Wylie, B. J., Borcik, C. G., and Khatib, S. J. (2020). "Bimetallic Mo-Co/ZSM-5 and Mo-Ni/ZSM-5 catalysts for methane dehydroaromatization: A study of the effect of pretreatment and metal loadings on the catalytic behavior," *Applied Catalysis A: General* 589, article no. 117247. DOI: 10.1016/j.apcata.2019.117247
- Wang, H., Ruan, H., Feng, M., Qin, Y., Job, H., Luo, L., Wang, C., Engelhard, M. H., Kuhn, E., Chen, X., Tucker, M. P., and Yang, B. (2017). "One-pot process for hydrodeoxygenation of lignin to alkanes using ru-based bimetallic and bifunctional catalysts supported on Zeolite Y," *ChemSusChem* 10(8), 1846-1856. DOI: 10.1002/cssc.201700160
- Wang, X., Du, B., Pu, L., Guo, Y., Li, H., and Zhou, J. (2018). "Effect of particle size of HZSM-5 zeolite on the catalytic depolymerization of organosolv lignin to phenols," *Journal of Analytical and Applied Pyrolysis* 129, 13-20. DOI: 10.1016/j.jaap.2017.12.011
- Wen, J.-L., Sun, S.-L., Yuan, T.-Q., Xu, F., and Sun, R.-C. (2013). "Structural elucidation of lignin polymers of eucalyptus chips during organosolv pretreatment and extended delignification," *Journal of Agricultural and Food Chemistry* 61(46), 11067-11075. DOI: 10.1021/jf403717q
- Ye, K., Liu, Y., Wu, S., and Zhuang, J. (2021). "A review for lignin valorization: Challenges and perspectives in catalytic hydrogenolysis," *Industrial Crops and Products* 172, 114008. DOI: 10.1016/j.indcrop.2021.114008
- Yu, J., He, D., Zhao, Y., Lu, J., Liu, J., Chen, D., Han, C., and Luo, Y. (2020). "Promotion of catalytic performance by adding chromium into HZSM-5 zeolite

- catalyst for methyl mercaptan catalytic conversion," *Materials Chemistry and Physics* 239, article no. 121952. DOI: 10.1016/j.matchemphys.2019.121952
- Yu, Y., Li, X., Su, L., Zhang, Y., Wang, Y., and Zhang, H. (2012). "The role of shape selectivity in catalytic fast pyrolysis of lignin with zeolite catalysts," *Applied Catalysis A: General* 447-448, 115-123. DOI: 10.1016/j.apcata.2012.09.012
- Zakzeski, J., Bruijninx, P. C. A., Jongerius, A. L., and Weckhuysen, B. M. (2010). "The catalytic valorization of lignin for the production of renewable chemicals," *Chemical Reviews* 110(6), 3552-3599. DOI: 10.1021/cr900354u
- Zeng, Z., Xie, J., Guo, Y., Rao, R., Chen, B., Cheng, L., Xie, Y., and Ouyang, X. (2021). "Hydrogenolysis of lignin to produce aromatic monomers over FePd bimetallic catalyst supported on HZSM-5," *Fuel Processing Technology* 213, article no. 106713. DOI: 10.1016/j.fuproc.2020.106713
- Zhai, Y., Li, C., Xu, G., Ma, Y., Liu, X., and Zhang, Y. (2017). "Depolymerization of lignin via a non-precious Ni-Fe alloy catalyst supported on activated carbon," *Green Chemistry* 19(8), 1895-1903. DOI: 10.1039/C7GC00149E
- Zhang, X., Ma, H., and Wu, S. (2020). "Effects of temperature and atmosphere on the formation of oligomers during the pyrolysis of lignin," *Fuel* 268, article no. 117328. DOI: 10.1016/j.fuel.2020.117328

Article submitted: December 25, 2021; Peer review completed: February 5, 2022;  
Revised version received: February 17, 2022; Accepted: February 18, 2022; Published:  
February 25, 2022.

DOI: 10.15376/biores.17.2.2275-2295